

pogenic driver, it becomes crucial to constantly monitor the world's most climatically sensitive areas. Examples of such areas include glaciers and ice sheets whose record melting is impacting communities on a global scale. In some cases, regions that rely upon glacial water as a principle source of fresh water are witnessing the rapid dwindling of resources. In other cases, rising sea level, to which the melting of glacier ice contributes, is threatening low-lying communities. Unfortunately, as is the case with the Greenland ice sheet, many such areas are remote and dangerous, making spatially and temporally comprehensive field measurements cost prohibitive. Hence, we must rely on remotely sensed measurements from aircraft and satellites in order to fill in our knowledge gaps left by sparse field measurements.

The Multi-angle Imaging SpectroRadiometer (MISR) instrument (operational since 2000) is on board the Earth Observing System (EOS) satellite, Terra, which is in a sun-synchronous polar orbit. MISR is uniquely suited for studying the poles because of the continuous, overlapping coverage of data taken by its nine pushbroom cameras that are arrayed at fixed angles ranging from  $0^\circ$  to  $70.5^\circ$  (from nadir) and symmetric about the nadir camera. Each camera has four filters: red, green, and blue (in the visible), and a near-infrared (NIR) at 866 micrometer ( $\mu\text{m}$ ) wavelength. The multi-angle views in conjunction with the 275-meter (m) resolution (available at the visible red wavelength on all nine cameras) can be used to compute a proxy of surface roughness of the observed target on a scale that is comparable to that of the Moderate Resolution Imaging Spectroradiometer (MODIS) 250-m data (Nolin and others, 2002). We have elected to use MISR's red-filtered C-cameras ( $60.0^\circ$  fore and aft) in order to define and investigate a proxy for ice surface roughness based on forward and backward scattered radiation, which we call the Normalized Difference Angular Index (NDAI). We define NDAI for Greenland to be fore C-camera red-channel values subtracted from the aft C-camera red-channel values divided by their sum. Because the forward-viewing camera is seeing forward-scattering radiation while the aft camera sees backscattered radiation (the sun is to the south), the forward scattering is associated with generally smooth surfaces and backward scattering dominates when an observed surface is rough (Nolin and Payne, 2007). Therefore, in an NDAI image, values range from -1 to 1 and rougher surfaces appear brighter.

As a case study of the NDAI proxy measurement, we chose to study a region in western Greenland encompassing Jakobshavn Glacier ( $69.2^\circ$  N,  $50.2^\circ$  W, 40 m elevation), which is one of the fastest moving glaciers in the world and one that drains a significant percentage of the Greenland ice sheet. Its area is greater than 9,200 square kilometers ( $\text{km}^2$ ) (Rignot and Kanagaratnam, 2006). Our study site extends upglacier in the inland ice to Summit ( $72.6^\circ$  N,  $38.5^\circ$  W, 3200 m elevation), which is the highest point on the Greenland ice sheet. We reviewed all available MISR images of the Greenland ice sheet for blocks 30 to 35, paths 8 to 10 during the 2000 to 2007 sunlit seasons across this transect. We determined 2004 to be the year when our study site was least obscured by clouds.

## Using Remote Sensing and GIS Techniques to Monitor the State of the Greenland Ice Sheet

By Meredith C. Payne<sup>1</sup> and Anne W. Nolin<sup>2</sup>

<sup>1</sup>College of Oceanic and Atmospheric Sciences, Oregon State University, Corvallis, Oreg.

<sup>2</sup>Department of Geosciences, Oregon State University, Corvallis, Oreg.

As we strive to tailor hypotheses related to global climate change while assessing the possibility of an anthro-

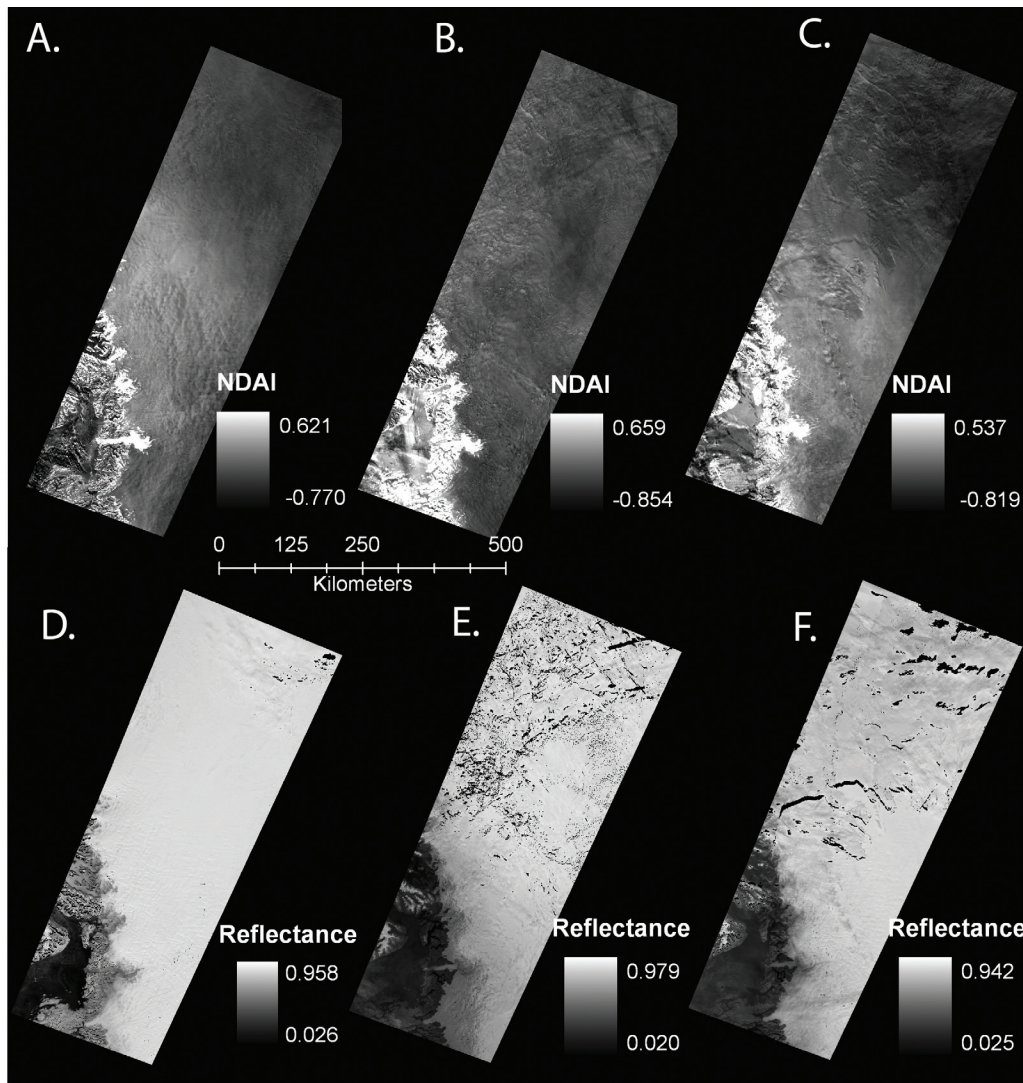


**Figure 1.** Images showing the ice-surface roughness of a portion of the Greenland ice sheet. Images A through C show the Normalized Difference Angular Index (NDAI), a proxy for ice-surface roughness, for the 2004 ablation season (April-May, June-July, and August-September composites, respectively). Higher NDAI values signify rougher surfaces. Images D through F are the composite reflectance images for April-May, June-July, and August-September, respectively. In images D through F, greater reflectance values signify smoother surfaces, which demonstrates the opposite relationship to the NDAI. Black pixels on the inland ice in images D through F indicate no data.

Nevertheless, completely cloud-free images over the entire region of study were impossible to come by. We investigated the application of the Radiometric Camera-by-camera Cloud Mask (RCCM) product, provided by the National Aeronautics and Space Administration's (NASA) Langley Atmospheric Science Data Center (ASDC) to the radiance images, but found the mask to be overly strict when distinguishing cloud pixels from ice pixels. Hence, using digital image processing along with geographic information system (GIS) techniques, we devised a method of creating composite images of NDAI and of top of the atmosphere (TOA) bidirectional reflectance factor (BRF) encompassing the early- (April and May), mid- (June and July), and late- (August and September) ablation season (fig. 1). These composite NDAI and reflectance images, along with their corresponding gradient images (mid-season composite minus early-season composite, and late-season composite minus mid-season composite) were examined to establish a pattern whereby the coastal regions are observed to grow progressively rougher throughout the ablation season. Ice surface roughness is intensified by (1) seasonal snow and ice in the ablation zone melting back to reveal underlying bed-

rock, (2) melt ponds forming upglacier in the wet-snow (slush) and percolation zones (as defined by Benson, 1960; Long and Drinkwater, 1994), (3) sastrugi (jagged erosional features caused by wind) morphology becoming more pronounced, and (4) melting and collapse of snow and ice bridges to reveal the highly irregular crevasse topography beneath. Although changes are not as dramatic upglacier towards Summit (melt ponds do not appear in the dry-snow zones), changes towards a rougher surface are observed mid-season in the percolation-zone, as NDAI pixels have greater values and become brighter compared with the early-season. As expected, there is little observed change in the near proximity of Summit over the sunlit season because it lies in the conjectured dry-snow zone as defined by Benson (1960) and Long and Drinkwater (1994). In the late-season images (August and September) after snowfall has resumed (especially over the wet-snow and percolation zones), NDAI values are observed to drop, but not fall as low as the early-season (April and May) values. Study of TOA reflectance images reveals the exact opposite relationship of pixel values throughout the time series: the pixels become darker (lower values) during mid-season and brighten

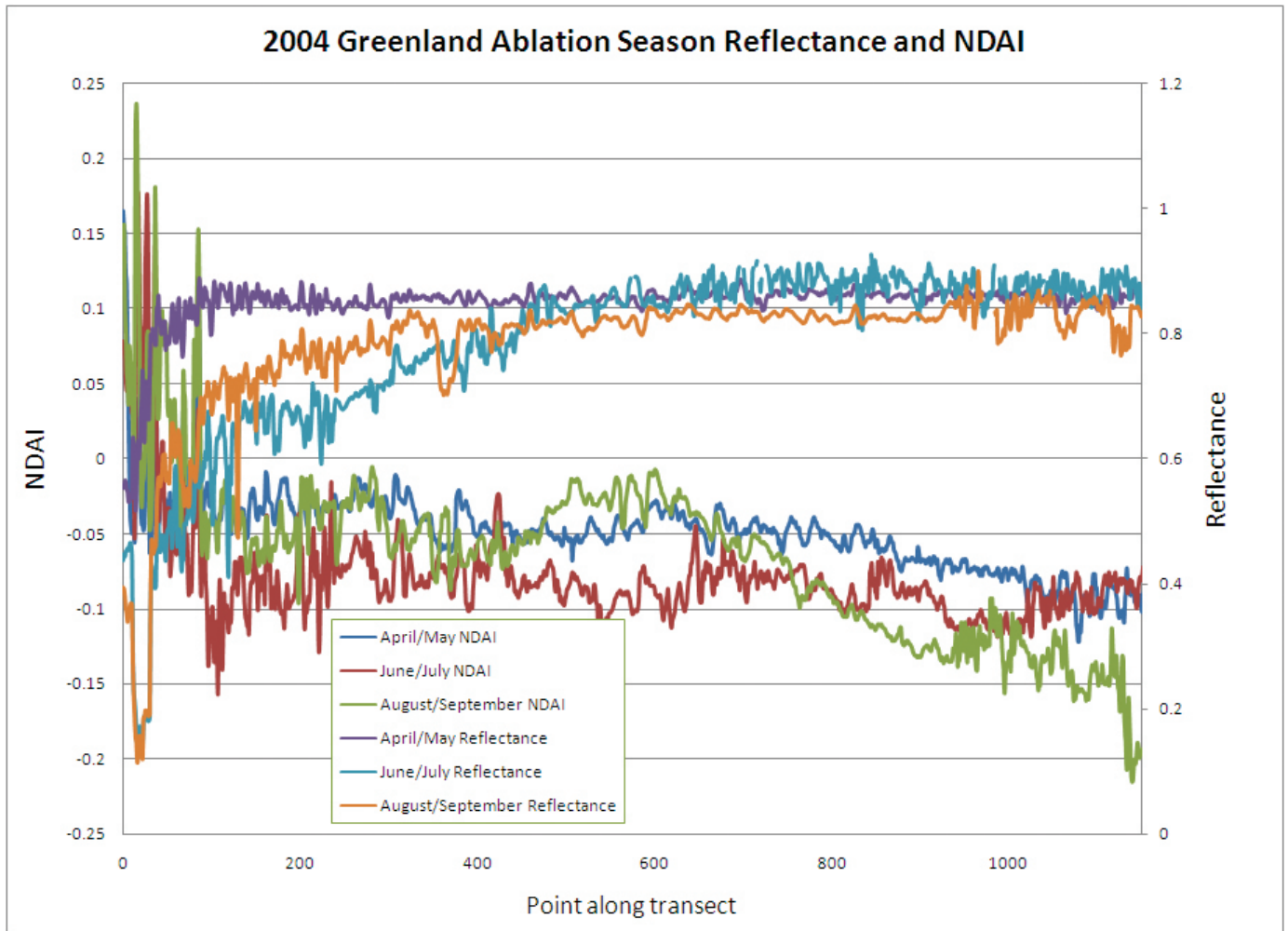


**Figure 2.** Graph showing Normalized Difference Angular Index (NDAI) values (left vertical axis) and reflectance values (right vertical axis) along a straight-line transect from Jakobshavn (left side of plot) to Summit (right side of plot) for the April-May, June-July, and August-September images as shown in figure 1. The contrasting relationship between NDAI and reflectance is noticeable, as is the trend of the ice surface growing rougher from spring to late summer, and then becoming smoother during late summer and early fall when snowfall recommences.

after fresh snowfall towards the end of the sunlit season. These relationships are illustrated in figure 2, in which NDAI and reflectance values from each of the three respective composite images are plotted along a straight transect from Jakobshavn to Summit.

We are encouraged enough by these results to proceed with production of similar NDAI composite images for the entire Greenland ice sheet for all years where enough low-cloud-percentage images are available. We hope to use these products to expand our analyses of the evolution of glacier zones during the operational lifetime of the MISR instrument to possibly include identification of glacier zones (such as the superimposed-ice zone) that are invisible to radar (Nolin and Payne, 2007). Furthermore, we believe that these products will enrich the already plentiful MISR dataset, which is publicly available for use in analyses.

## References Cited

- Benson, C.S., 1960, Stratigraphic studies in the snow and firn of the Greenland ice sheet: Pasadena, Calif., California Institute of Technology, unpublished Ph.D. dissertation, 213 p.
- Long, D.L., and Drinkwater, M.R., 1994, Greenland observed at high resolution by the Seasat-A scatterometer: *Journal of Glaciology*, v. 40, p. 213–220.
- Nolin, A.W., Fetterer, F.M., and Scambos, T.A., 2002, Surface roughness characterizations of sea ice and ice sheets—Case studies with MISR data: *IEEE Transactions on Geoscience and Remote Sensing*, v. 40, p. 1,605–1,615.

## 6 Geoinformatics 2008—Data to Knowledge

Nolin, A.W., and Payne, M.C., 2007, Classification of glacier zones in western Greenland using albedo and surface roughness from the Multi-angle Imaging SpectroRadiometer (MISR): *Remote Sensing of Environment*, v. 107, p. 264–275.

Rignot, E., and Kanagaratnam, P., 2006, Changes in the velocity structure of the Greenland ice sheet: *Science*, v. 311, p. 986–990.